



---

## Figures and figure supplements

Phloem unloading in *Arabidopsis* roots is convective and regulated by the phloem-pole pericycle

**Timothy J Ross-Elliott *et al***

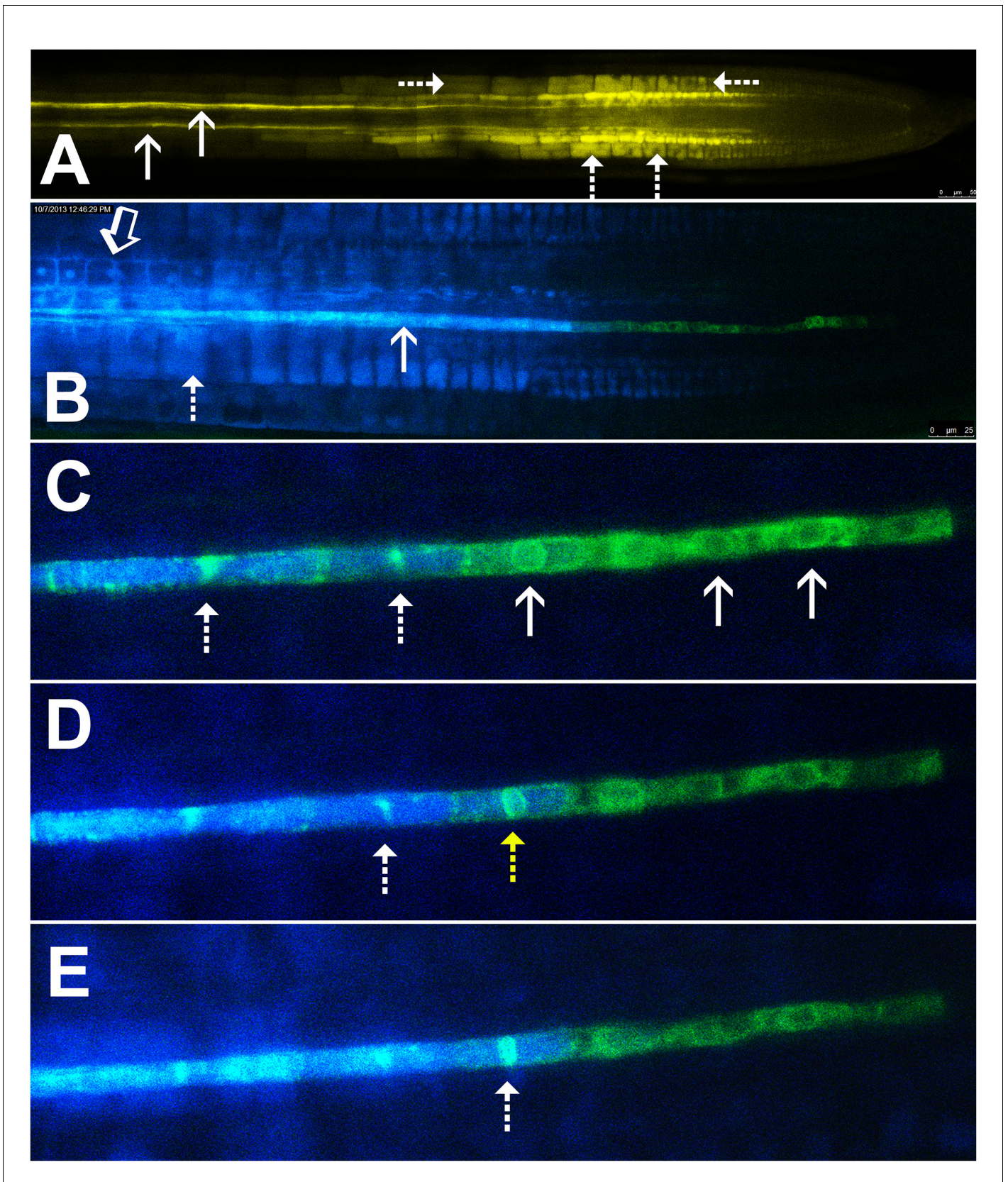


**Figure 1.** Symplastic unloading of phloem mobile probes. (A) 2D optical section of unloading of CFDA in the root tip. The two protophloem files leading into the root tip are shown (solid arrows) and sequestration of CFDA into the vacuoles is apparent (dashed arrows). (B) Unloading of esculin  
 Figure 1 continued on next page

*Figure 1 continued*

(blue) in the root tip of a transgenic *Arabidopsis* line expressing GFP (green) targeted to the ER lumen of the PSE (pMtSEO2::GFP5-ER). Esculin escapes the protophloem file (solid arrow) into the cytoplasm of neighboring cells (open arrow). In contrast to CFDA, esculin is only sequestered in the vacuoles at high concentrations (dashed arrow). (C–E) Three frames extracted from **Video 1**. (C) GFP targeted to the ER lumen of PSEs demarcates the nuclear membrane of young sieve elements that have not yet been integrated into the unloading zone (solid arrows). Dashed arrows indicate two degrading nuclei in cells that are already filled with esculin (blue) (also for D and E). (D) Degradation of the nucleus (yellow arrow) coincides with the opening of the sieve-plate pores, allowing esculin (blue) to enter the cell. This defines the new PSE zero. (E) As nuclear degradation continues, the sieve element becomes an integral member of the phloem unloading zone.

DOI: [10.7554/eLife.24125.003](https://doi.org/10.7554/eLife.24125.003)

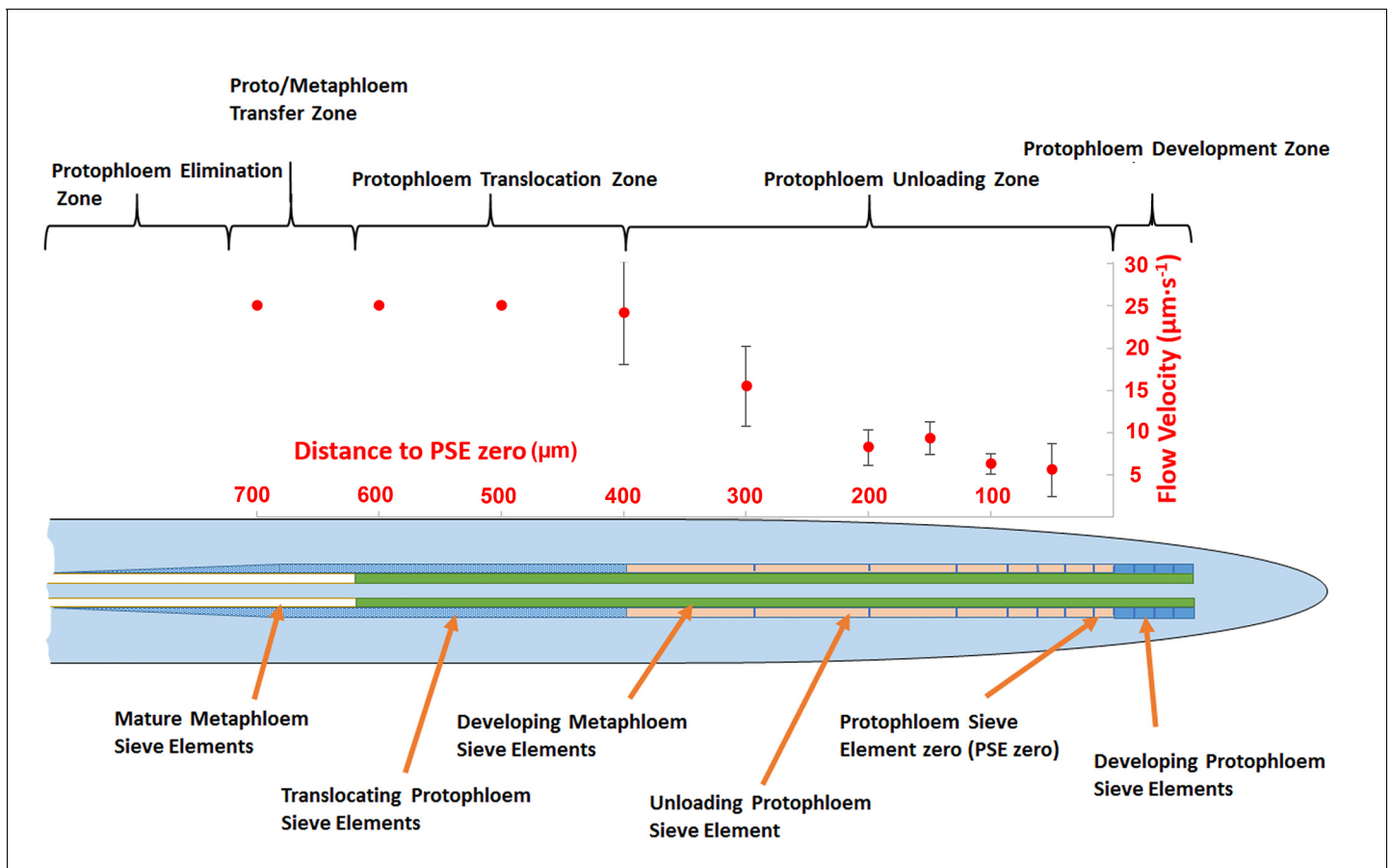


**Figure 2.** Schematic diagram illustrating the organization of phloem cells in specific zones in the root tip of Arabidopsis. The graph represents experimentally derived velocities at defined points relative to the terminal sieve element (PSE zero) in the protophloem unloading zone. Error bars show standard deviation of the mean ( $n = 8$ ).

DOI: [10.7554/eLife.24125.005](https://doi.org/10.7554/eLife.24125.005)

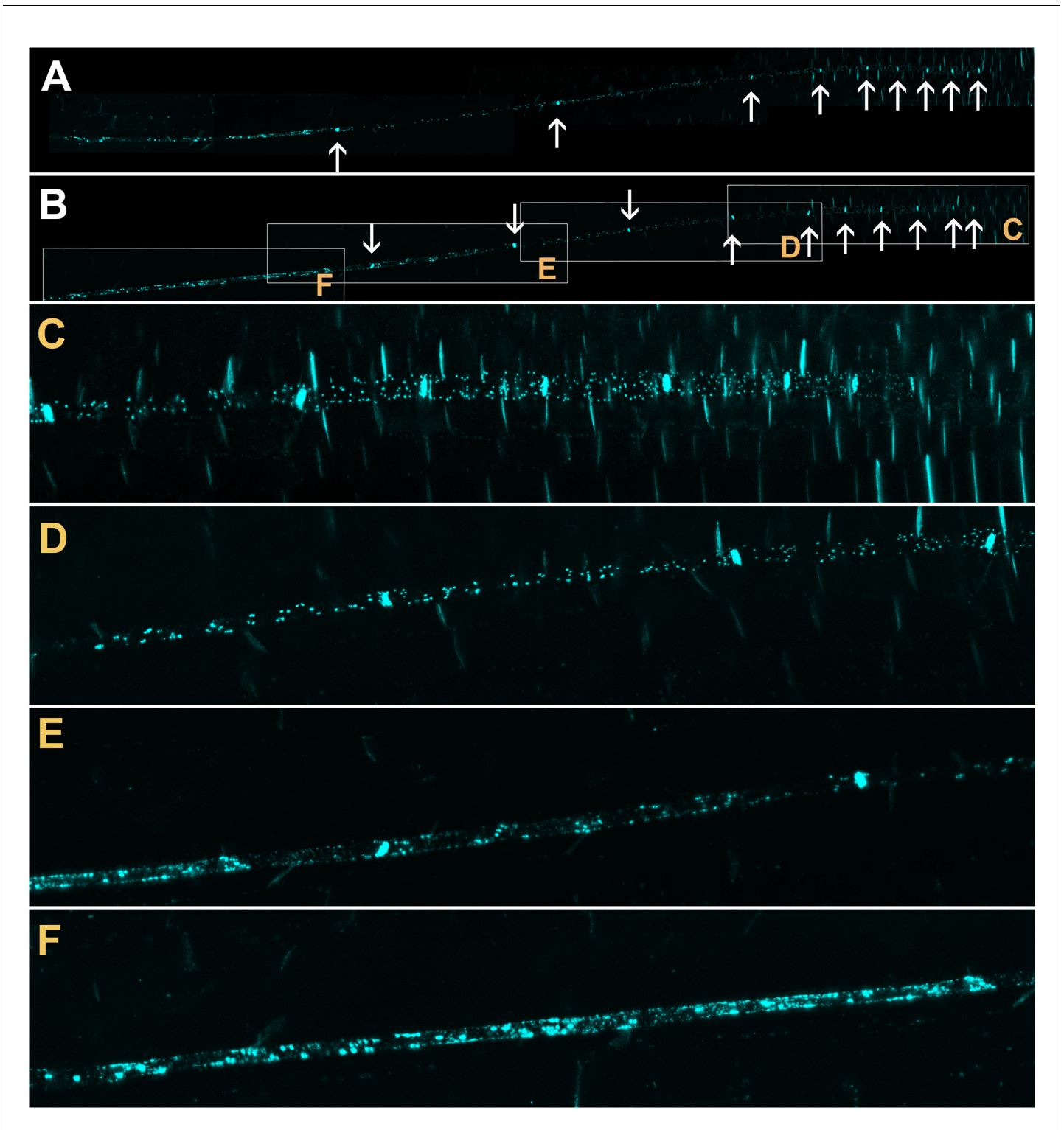


**Figure 3.** Confocal micrographs of the unloading zone in the Arabidopsis root tip stained with Sirofluor. Low magnification images showing the relatively strong fluorescence at sieve plates (arrows). (C–F) Higher magnification images at the locations indicated by boxes in (B). Individual plasmodesmata are resolved in the unloading zone (C, D). In the translocation zone, large deposits of callose are abundant (E, F).

DOI: [10.7554/eLife.24125.006](https://doi.org/10.7554/eLife.24125.006)

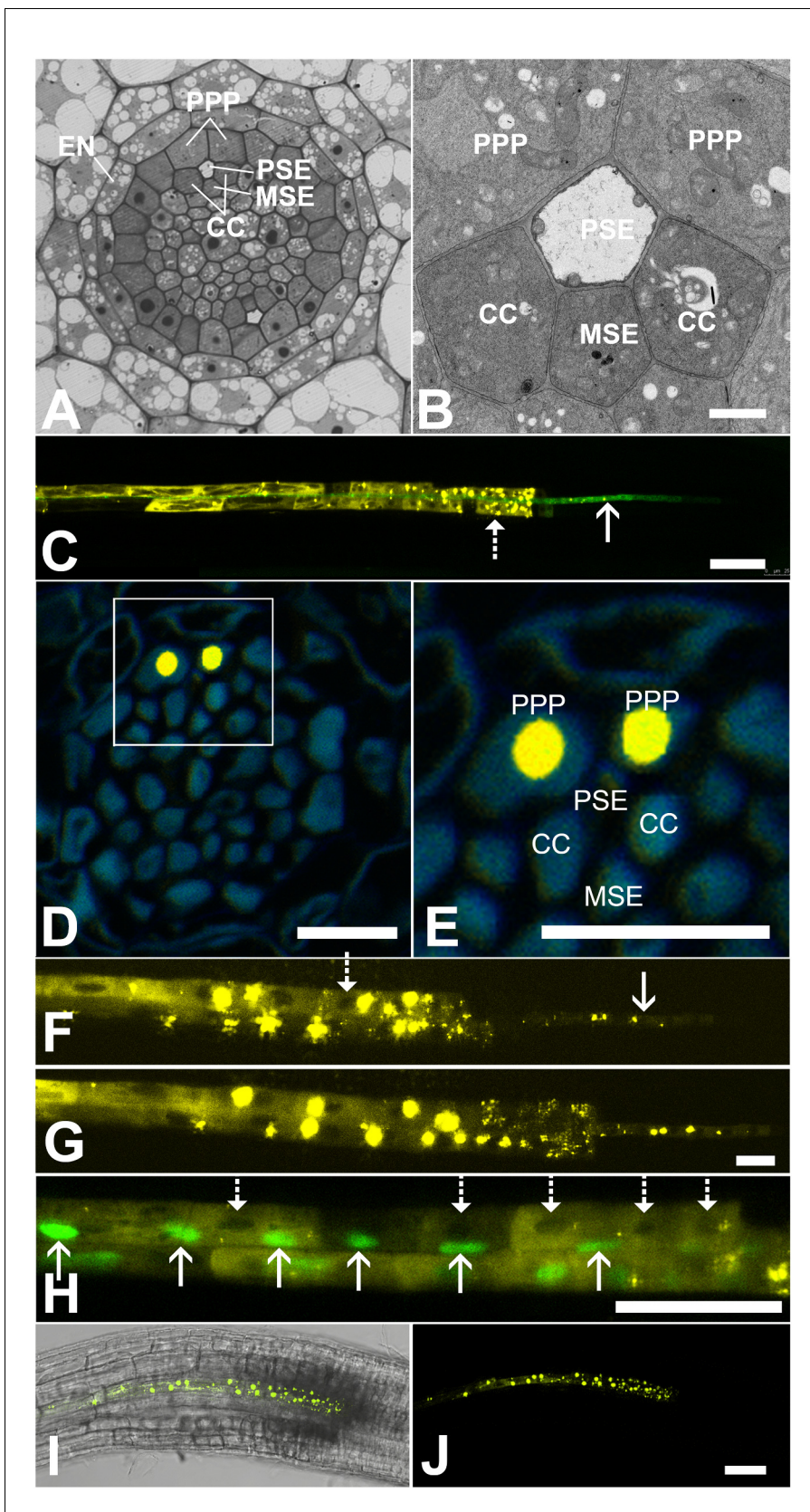


**Figure 4.** Functional organization in the root unloading zone. (A, B) TEM images showing a cross section of an Arabidopsis root unloading zone. (A) An overview of the central cylinder with phloem pole pericycle cells (PPP), endodermis (EN), companion cells (CC), metaphloem sieve element (MSE), and phloem sieve element (PSE). (B) Higher magnification of the unloading zone. (C) Fluorescence image showing yellow and green signals. (D) Fluorescence image with a white box indicating the area in E. (E) Fluorescence image showing yellow signals in PPP cells and blue signals in PSE, CC, and MSE cells. (F) Fluorescence image showing yellow signals. (G) Fluorescence image showing yellow signals. (H) Fluorescence image showing green signals. (I) Fluorescence image of a root section. (J) Fluorescence image of a root section. *Figure 4 continued on next page*

*Figure 4 continued*

protophloem sieve element (PSE). (B) TEM image of the pentagonal organization of cells surrounding the protophloem file. (C) Confocal micrograph of a transgenic *Arabidopsis* line expressing SEOR-YFP protein (yellow) and GFP targeted to the sieve element ER (green), both under control under a sieve element specific promoter. While GFP is restricted to the ER of the PSE (solid arrow), SEOR-YFP expressed into the cytoplasm escapes into two neighboring cell files (dashed arrow). (D, E) Root cross section of a fixed and embedded transgenic *Arabidopsis* plant expressing SEOR-YFP protein. The micrograph identifies the two cell files into which SEOR-YFP escapes as the PPP. (F, G) Two confocal micrographs extracted from **Video 2** showing SEOR-YFP protein (yellow) in the PPP and PSE. New PPP cells become fluorescent as unloading progresses. Note that small aggregates of SEOR-YFP become increasingly larger basipetal to the unloading zone. (H) Confocal micrograph of a transgenic *Arabidopsis* line expressing GFP (green) in the nuclei of companion cells (solid arrows) and SEOR-YFP. The nuclei in the CCs do not match the location of the nuclei in the cell files containing SEOR-YFP (dashed arrows), providing further evidence that the two files are the PPP. (I, J) Root tip of a grafted *Arabidopsis* plant in which the rootstock was wildtype and the scion expressed SEOR-YFP in the shoot. The root was imaged at 10 days after grafting and shows clearly that SEOR-YFP protein has moved from shoot to root, with subsequent unloading into the PPP. Scale Bars; B = 1  $\mu\text{m}$ ; F, G = 5  $\mu\text{m}$ ; C, D, E, H = 10  $\mu\text{m}$ ; I, J = 50  $\mu\text{m}$ .

DOI: [10.7554/eLife.24125.007](https://doi.org/10.7554/eLife.24125.007)

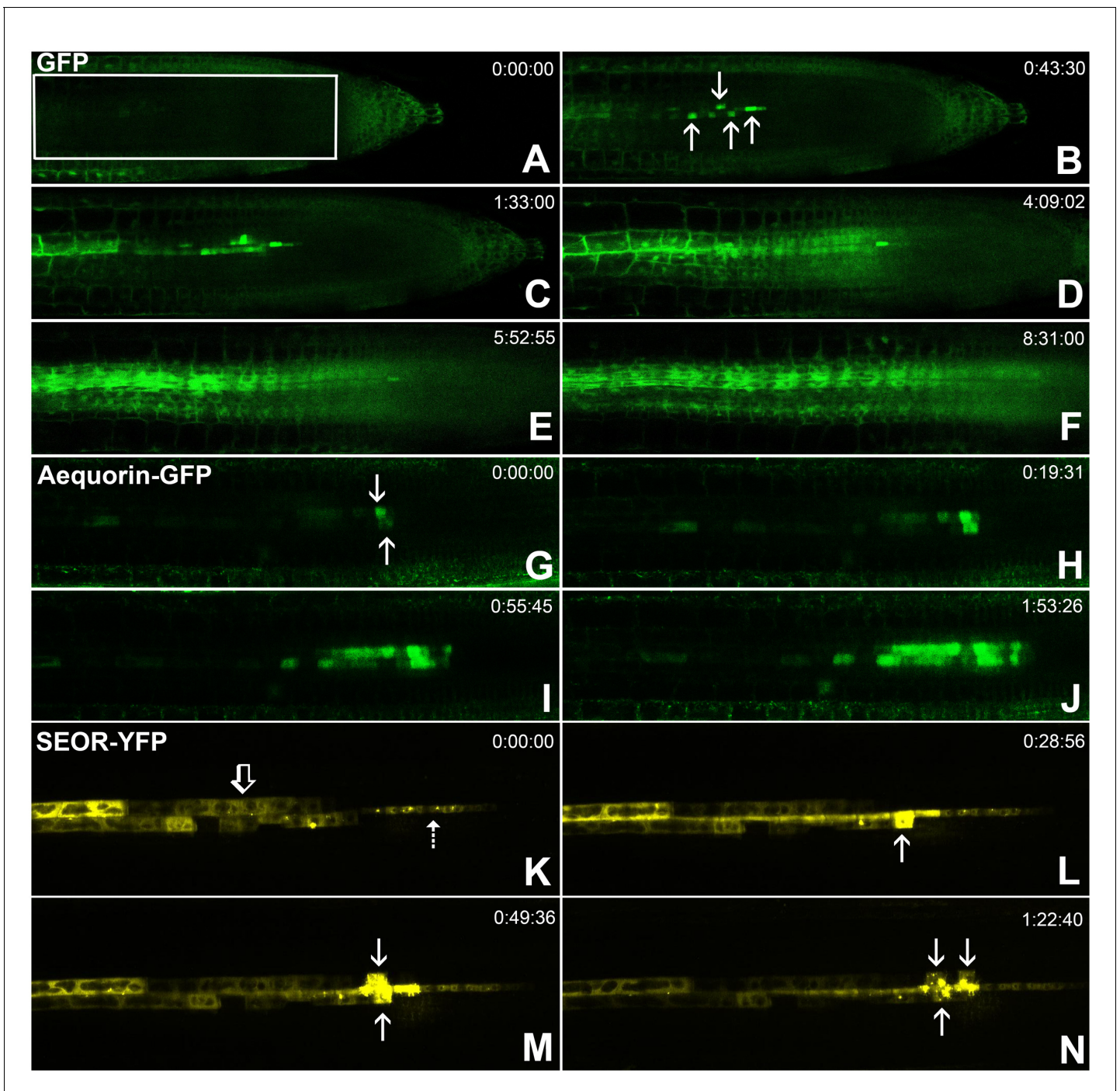


**Figure 5.** Batch unloading of proteins. (A–F) six frames taken from **Video 3**. A) The unloading zone was photobleached (boxed region). Refilling of the unloading zone shows that GFP exits the PSE in discrete batches (arrows in B). Over time, all cells in the root transported GFP until an even distribution of the fluorescent protein was reinstated (C–F). (G–J) Compared to GFP (27 kDa), aequorin-GFP (48 kDa) was batch unloaded but did not move beyond the PPP. (K–N) Four frames extracted from **Video 4** showing batch unloading of SEOR-YFP (112 kDa). In contrast to the CC-expressed GFP probes, SEOR-YFP was expressed in young sieve elements and entered the translocation stream when the sieve-plate pores opened. The immature PSEs are indicated (dashed arrow) and PPP cells are visible (open arrow). When SEOR-YFP aggregates arrive in the phloem unloading zone, they are batch unloaded from the terminal PSEs (solid arrows). As the root continues to extend, the aggregates enlarge and eventually disappear (see also **Figure 4F, G** and **Videos 2** and **4**), probably due to their breakdown in the older PPP cells.

DOI: [10.7554/eLife.24125.008](https://doi.org/10.7554/eLife.24125.008)

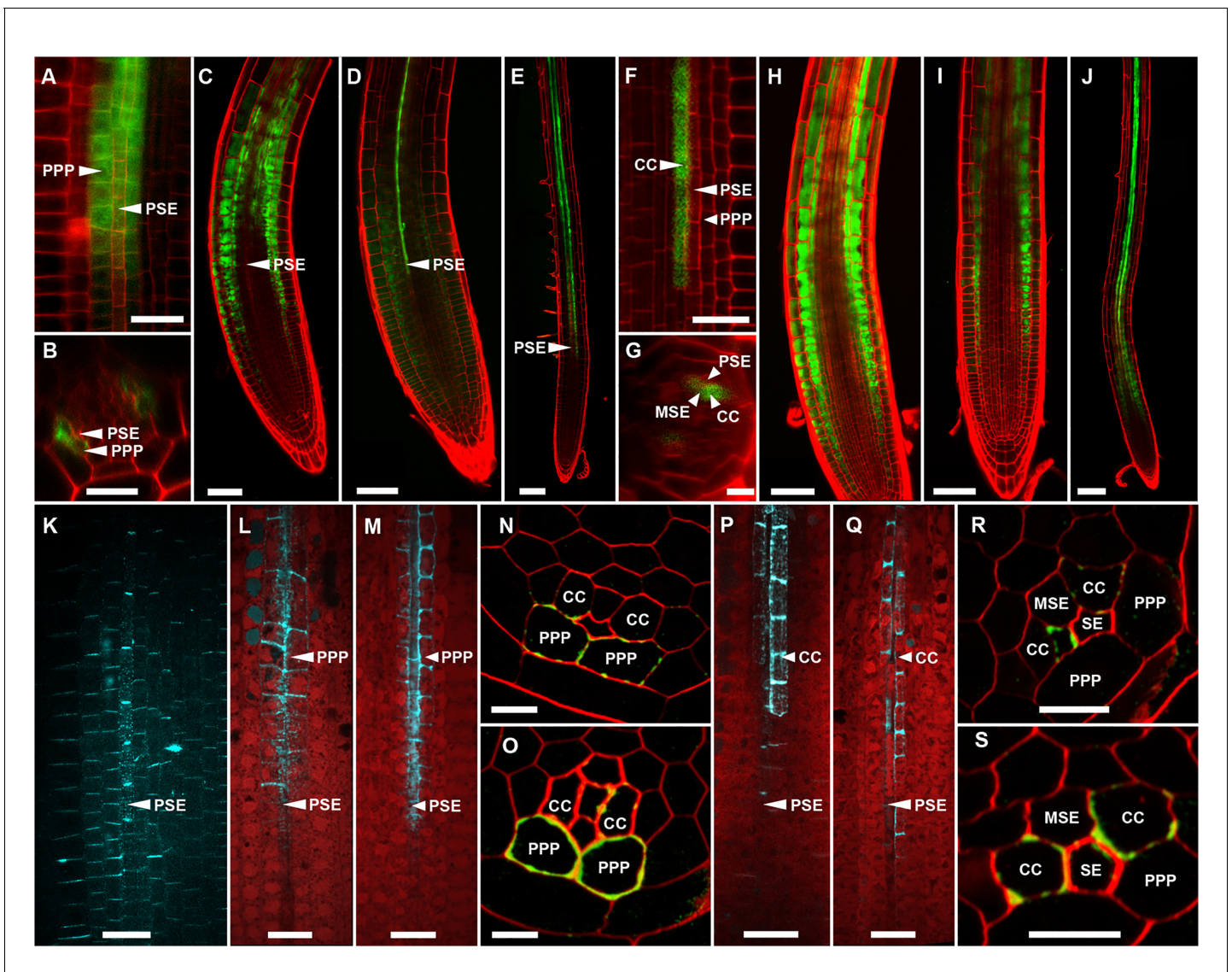


**Figure 6.** Callose induction in the PPP, but not CCs, blocks phloem unloading. (A) *pCALS8::ER-YFP* is expressed exclusively in the PPP. (B) Transverse optical section of A. (C) CF unloading in a control root expressing *pCALS8::icals3m* transferred to non-inducing medium. Unloading progresses as in wild-type roots. (D) CF unloading is restricted to the PSE files in *pCALS8::icals3m* roots at 8 hr after callose induction in the PPP. (E) As D but at 24 hr post-callose induction in the PPP. (F) *psAPL* promoter expression (*psAPL-GFP*) is restricted to CCs and MSE. (G) Transverse optical section of F. (H) CF unloading in a control root expressing *psAPL::icals3m* transferred to non-inducing medium. (I) CF unloading is not restricted in *psAPL::icals3m* roots at 8 hr after callose induction in CCs. (J) As I but at 24 hr post-callose induction in CCs. (K) Sirofluor staining of a control root showing general background staining of PD around PSE files. (L) Sirofluor staining of a *pCALS8::icals3m* root at 8 hr after callose induction in the PPP. (M) Sirofluor staining of a *pCALS8::icals3m* root at 24 hr after callose induction. In both L and M the roots were stained immediately after CF transport. (N) Callose immunolabelling (green) of a *pCALS8::icals3m* root at 8 hr after callose induction in the PPP. Cell walls are labelled red. (O) As N but at 24 hr after callose induction. (In addition to the PPP, sometimes callose staining is also observed in the CC). (P) Sirofluor staining of a *psAPL::icals3m* root at 8 hr after callose induction in CCs. (Q) As P but at 24 hr after callose induction. (R) Callose immunolabelling (green) of a *psAPL::icals3m* root at 8 hr after callose induction in CCs. (In addition to the CC, callose staining was sometimes observed in the MSE). Cell walls were counterstained with calcofluor white (labelled red). (S) As R but at 24 hr after callose induction. Scale bars: N, O, R, S: 5  $\mu$ m. A, B, F, G, K, L, M, P, Q: 10  $\mu$ m. C, D, H, I, J: 50  $\mu$ m. E, J: 100  $\mu$ m. Abbreviations as in **Figure 4**.

DOI: [10.7554/eLife.24125.011](https://doi.org/10.7554/eLife.24125.011)

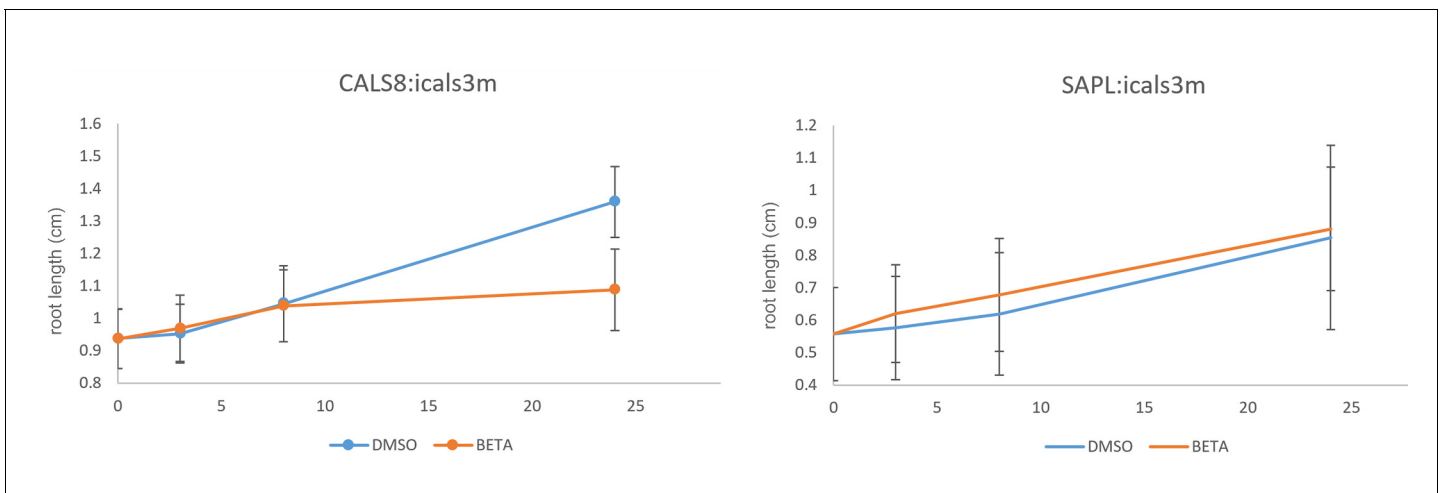


**Figure 6—figure supplement 1.** Growth of *pCALS8::icals3m* and *psAPL::icals3m* seedlings on 5  $\mu$ M beta estradiol relative to uninduced controls (mock DMSO). Seedlings were transferred to inducing or non-inducing media at 4 days post germination. For *pCALS8::icals3m* each time point is the average of 82 independent measurements. For *psAPL::icals3m* each time point is the average of 67 independent measurements. Bars show standard error of the mean.

DOI: [10.7554/eLife.24125.012](https://doi.org/10.7554/eLife.24125.012)

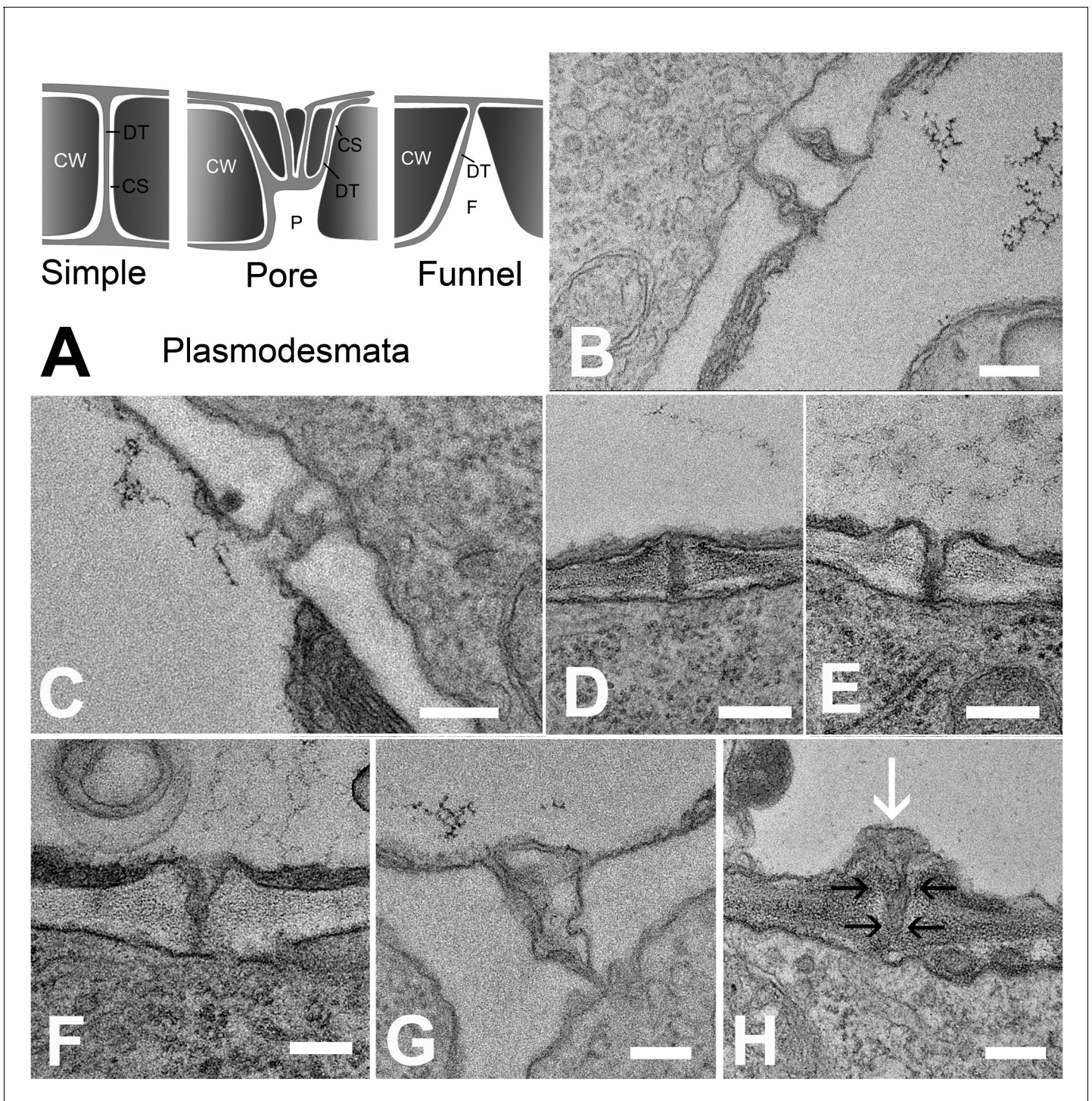


**Figure 7.** Types of plasmodesmata connecting different cell interfaces. (A) Schematic diagrams of the different plasmodesmata connecting protophloem sieve elements to surrounding cell types. (B) Image of the PSE-MSE interface showing a cell wall with two simple plasmodesmata. (C) A pore-plasmodesma in the cell wall between PSE and CC. (D–I) Plasmodesmata connecting PSE with PPP. (D) Simple plasmodesmata, found rarely. (E–H) Funnel plasmodesmata. These showed a wide opening on the PSE entrance tapering towards the PPP. (H) Electron-dense components (white arrow) of unknown composition were often observed within funnel plasmodesmata (black arrows). DT = desmotubule, CW = cell wall, P = pore, F = funnel, CS = cytoplasmic sleeve. Scale bars: B, C, G, H = 200 nm; D, E, F = 500 nm.

DOI: [10.7554/eLife.24125.013](https://doi.org/10.7554/eLife.24125.013)

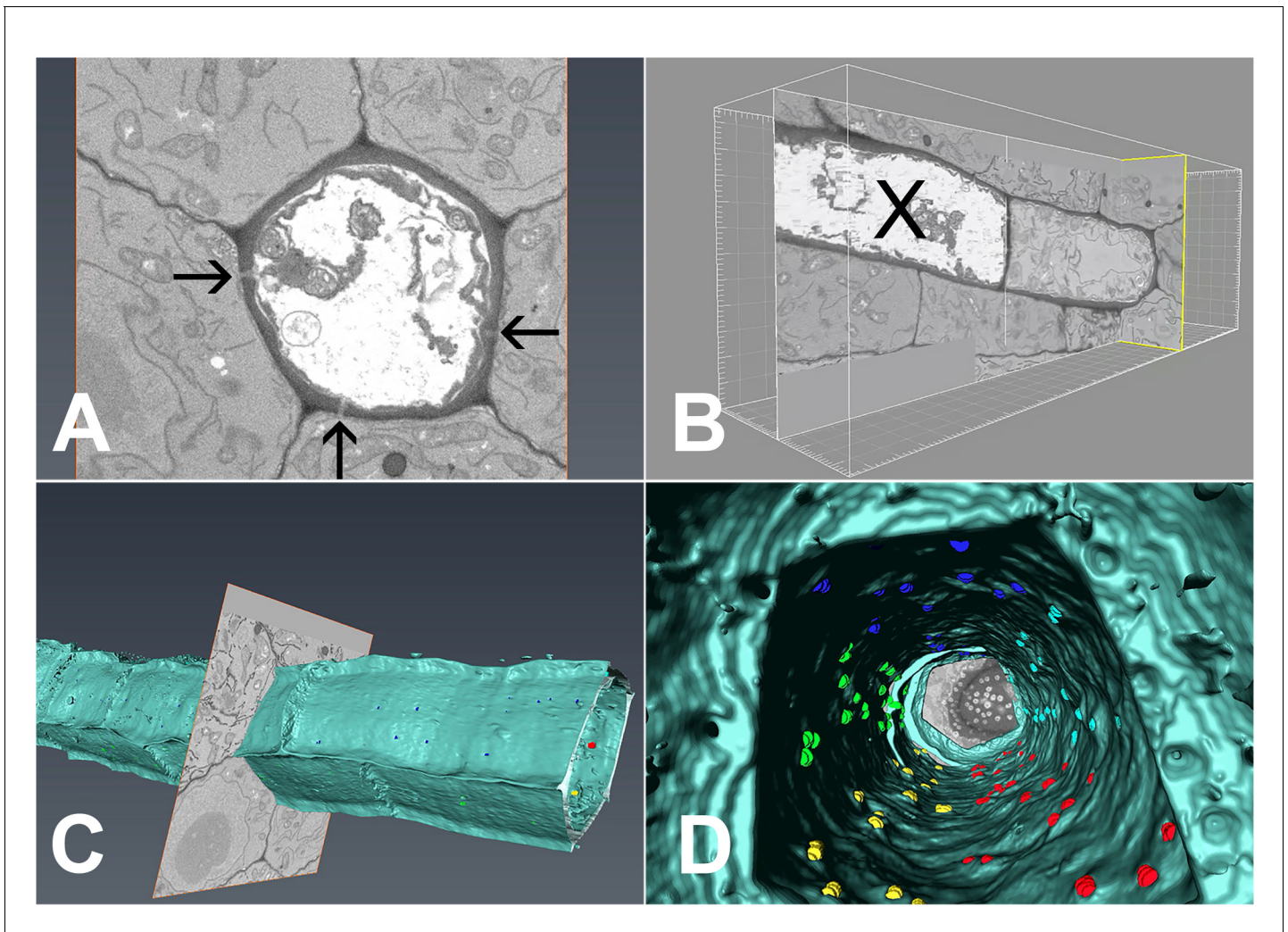


**Figure 8.** 3D overview of protophloem sieve elements in the root tip obtained by serial block-face scanning electron microscopy. (A) Cross-section of one phloem pole in the unloading zone. PD are indicated by darts. (B) Longitudinal section of the protophloem unloading zone. PSE zero (X) is connected to a neighboring immature protophloem sieve element. (C, D) 3D longitudinal view of the protophloem unloading zone. Serial sections were used to reconstruct the unloading zone and quantify PD connections from PSEs to adjacent cells. (C) shows PD on the outer face of the PSE. (D) is derived from [Video 4](#) and shows the PD on the inner faces of the PSE. In the images, PD are color coded (blue/cyan PSE-PPP, red/green PSE-CC, and yellow PSE-MSE).

DOI: [10.7554/eLife.24125.014](https://doi.org/10.7554/eLife.24125.014)

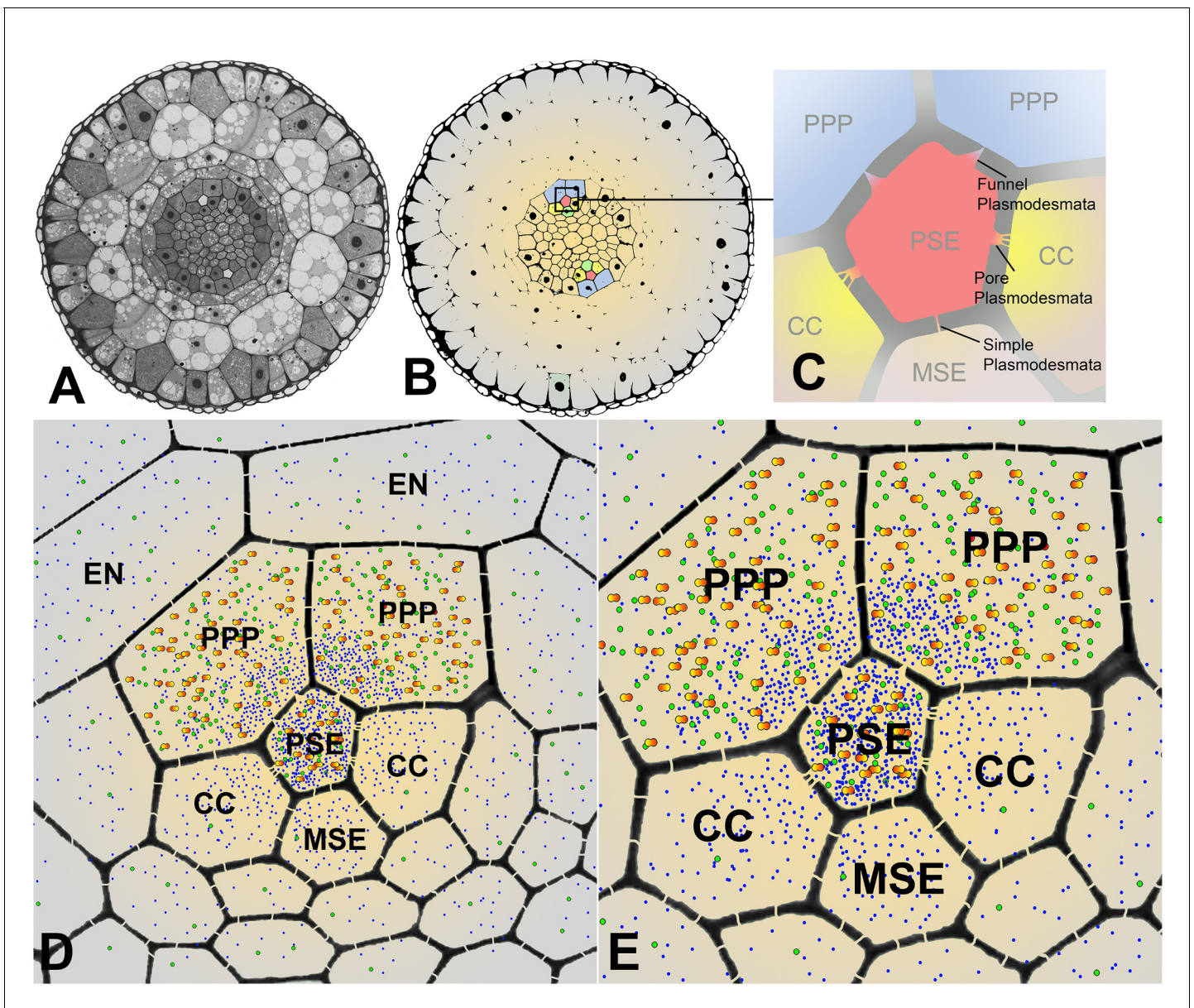
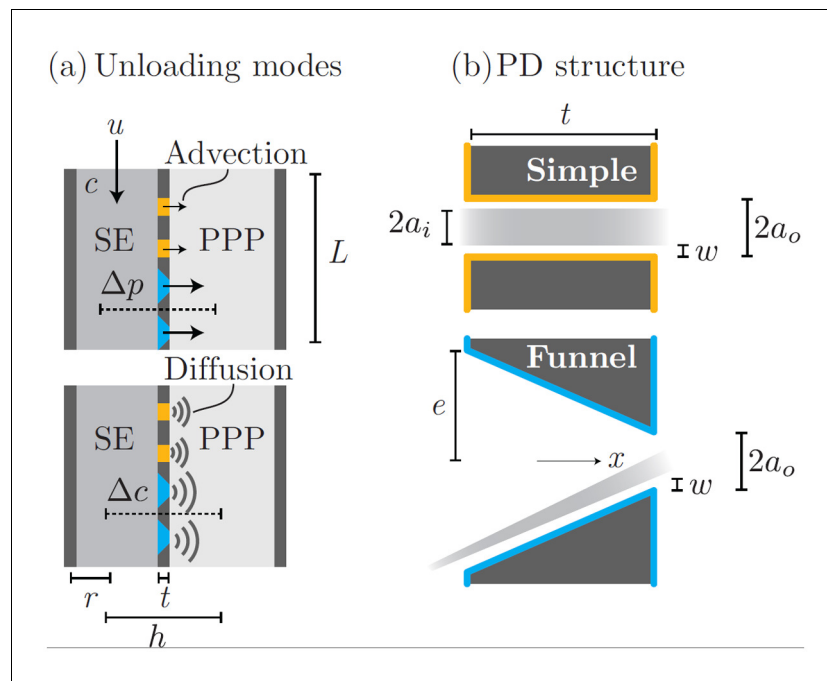


**Figure 9.** Cross sectional overviews of the Arabidopsis roots showing PD connections and size-dependent phloem unloading of solutes and macromolecules. (A) Standard light micrograph showing a cross section of the Arabidopsis root. (B) A false colored cross section of the Arabidopsis root highlighting the two phloem poles in the unloading zone. (C) Diagram of the cells in the phloem pole and the types of PD that connect the PSEs to each adjacent cell. PPP cells are connected to the PSE by funnel PD, CCs are connected by pore-PD, and MSEs are connected by simple PD. (D and E) Diagram showing the location of various solutes and macromolecules depending on molecular mass. Once unloaded via the PPP, sucrose (blue dots) and GFP (green dots) are able subsequently to enter all cell types via PD. However, larger macromolecules such as SEOR-YFP (yellow/orange dots) are unloaded only into PPP cells. EN = endodermis.  
DOI: [10.7554/eLife.24125.018](https://doi.org/10.7554/eLife.24125.018)



**Appendix 1—figure 1.** Phloem unloading model. Parameters used in calculations for advective and diffusive modes (a): bulk flow and diffusion through PD types (b): simple and funnel. See **Table 1** for parameter descriptions and values.

DOI: [10.7554/eLife.24125.020](https://doi.org/10.7554/eLife.24125.020)